STUDIA UBB CHEMIA, LXIII, 1, 2018 (p. 109-123)
(RECOMMENDED CITATION)
DOI:10.24193/subbchem.2018.1.09

A 250-YEAR ISOTOPIC PROXY RAINFALL RECORD FROM SOUTHERN BOTSWANA

STEPHAN WOODBORNE[a,b*], GRANT HALL[b], CONNOR W. JONES[c], NEIL J. LOADER[c], ADRIAN PATRUT[d], ROXANA T. PATRUT[d], IAIN ROBERTSON[c], STEPHAN R. WINKLER[a], CHRISTIAAN W. WINTERBACH[e]

ABSTRACT. Climate records along aridity gradients where manifestations of climate change are most profound are important for testing climate models. The *Kalahari Transect* spans such a gradient, but instrumental records of climate parameters are limited in the sparsely populated region. We analysed the $\delta^{13}C$ and $\delta^{18}O$ record from a *Vachellia erioloba* (E.Mey) tree from the southern Kalahari Desert in Botswana to explore its potential as a climate proxy archive. Radiocarbon dates show that the record spans the period 1758-2013 CE. Both the $\delta^{13}C$ and $\delta^{18}O$ records correlate with local rainfall. The isotope proxies show a weak positive correlation with sea-surface temperature reconstruction from the southwestern Indian Ocean, and a stronger correlation with the El Niño Southern Oscillation index. This appears to contradict previous evidence that higher sea-surface temperatures are associated with reduced summer rainfall over the southern African interior. Instead of eastward shifts in the temperate tropical trough synoptic system during elevated southwestern Indian Ocean temperature anomalies, the evidence supports a westwards shift. The result demonstrates the potential of *Vachellia erioloba* as a climate proxy archive that may yield past climate variability from the arid regions of southern Africa.

Keywords: *ENSO, drought, Southern Africa, AMS radiocarbon dating, Vachellia erioloba, oxygen isotopes, carbon isotopes.*

[a] *iThemba LABS, Private Bag 11, WITS 2050, South Africa.*
[b] *Mammal Research Institute, University of Pretoria, Private Bag X20, Hatfield 0028, South Africa.*
[c] *Swansea University, Department of Geography, Swansea SA2 8PP, UK.*
[d] *Babeş-Bolyai University, Faculty of Chemistry and Chemical Engineering, 11 Arany Janos, RO-400028, Cluj-Napoca, Romania.*
[e] *Tau Consultants (Pty) Ltd, P/Bag 83, Maun, Botswana.*
[*] *Corresponding author: swoodborne@tlabs.ac.za*

INTRODUCTION

The majority of the inhabitants of southern Africa are dependent on non-commercial rain-fed agricultural subsistence strategies [1]. A persistent threat to this economy is rainfall variability, and although the region experiences substantial droughts, the instrumental rainfall records that might elucidate the underlying forcing are generally of short duration. Attempts to understand wet/dry cycles in Botswana, for example, have relied on records as short as 30- [2] to 50- [3,4] years. Despite the poor instrumental records there is strong evidence for the role of the El Niño Southern Oscillation (ENSO) in mediating droughts [5], but the relationship is not linear. While most El Niño events are associated with droughts, some are associated with wetter conditions [6-8]. The ENSO phenomenon operates at an inter-annual time scale, but there is also evidence for large-scale synoptic changes that drive rainfall variability at near-decadal time scales. Since most of the moisture advected over the southern African continent comes from the southwestern Indian Ocean [9] the most likely large scale forcing is in response to sea-surface temperature changes (SWIO SST) in that region [5,10,11].

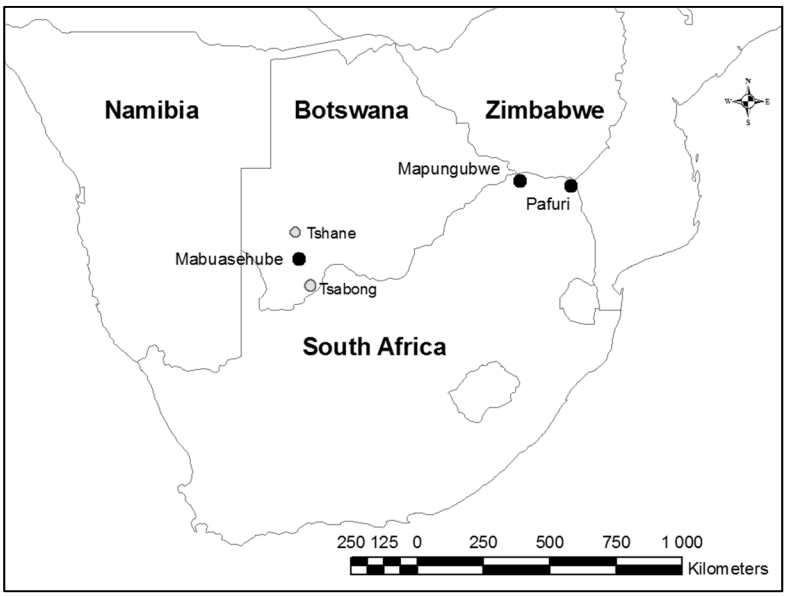

Figure 1. Map of the study region showing the location of tree sampling sites (black symbols) and towns (grey symbols) mentioned in the text.

The short- and long-term forcing mechanisms for rainfall over southern Africa may operate to reinforce or annul one another, and the net effect is that wet/dry cycles are not random, but instead seem to oscillate at a 16-20 year periodicity [12]. If an underlying driver of rainfall variability changes over longer periods (multi-decadal to centennial time scales) then the ability to discern the effect is severely limited owing to the short duration of the instrumental data. Not only is this relevant for understanding the return time of droughts, but it is very relevant to understand the mechanisms underlying projected future climate changes. Climate change forecasts suggest that parts of the study area will be among the fastest warming areas on Earth, and the same regions will also experience significant reductions in rainfall [13,14]. The vulnerability of communities and even the National GDP of countries to drought in southern Africa are likely to be exacerbated into the future. Testing the skill of climate forecasts is necessary, but the poor instrumental record is a strong constraint.

Southern Africa is characterized by strong climatic gradients between hot, dry deserts and more mesic regions. The ecological gradients have been studied in the context of ecosystem services along the *Kalahari Transect* [15], but they also offer sensitive indicators of climate change and climate forcing. Verification of forcing mechanisms requires longer time series for rainfall, which in the absence of good instrumental records, is often derived from tree ring analyses. Classic applications of ring width chronologies in southern Africa are rare [16-21] because few tree species have been shown to grow annual rings that record climate variability. Recent studies have made use of the correlation between leaf-level transpiration regulation and stable carbon isotope ratios ($\delta^{13}C$) in wood [11, 22-24] to generate proxy rainfall records. Most of this research focused on tree species that do not occur in the xeric regions. In this study we attempt to generate a climate record from a *Vachellia erioloba* tree from southern Botswana (**Figure 1**) using stable isotope proxies and a radiocarbon based age model. *Vachellia erioloba* is a cornerstone species in the arid regions and preliminary studies suggest that its sensitivity to environmental forcing (rainfall) and longevity [25], and its low sensitivity to intrinsic water-use efficiency changes with elevated CO_2 [26] make it a potentially valuable archive of climate variability.

RESULTS AND DISCUSSION

The age model suggests that the Mabuasehube *Vachellia erioloba* specimen died in approximately 2013 CE (**Figure 2**), - 2 years prior to sampling, which accords with its physical appearance. It started growing in approximately

1758 CE and so the radial section records the growth over the last 255 years. The implication of the age model is that sampling density is sub-annual (average 1.43 samples per year) post 1947 CE, and near biennial (average 0.52 samples per year) prior to 1947 CE.

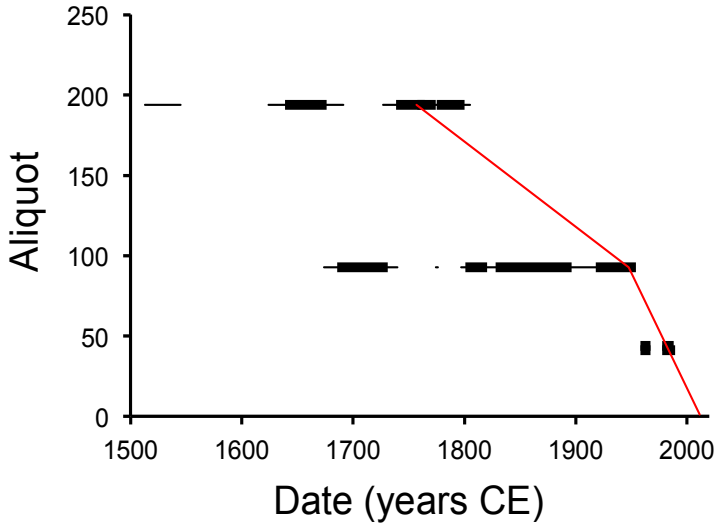

Figure 2. Age model for the Mabuasehube *Vachellia erioloba*. The 1-sigma calibrated intercept ranges for the four radiocarbon dates in Table 1 are represented by bold horizontal black lines while 2-sigma ranges are represented by thin horizontal black lines. The age model (red line) is a linear relationship between aliquot number (commencing with 0=bark) and calendar age with a gradient change at aliquot 93. The age model intercepts all the radiocarbon ages in the 1-sigma range.

The $\delta^{13}C$ and $\delta^{18}O$ isotopic time series are presented in **Figure 3**. In this representation the $\delta^{13}C$ y-axis is inverted because less negative/more positive values are associated with dry conditions, and more negative/less positive values with wetter conditions. An inverted $\delta^{13}C$ y-axis may intuitively be interpreted as a proxy rainfall scale. Since $\delta^{13}C$ and $\delta^{18}O$ co-vary ($r=0.424$, $p<0.001$, $n=142$), the y-axis for $\delta^{18}O$ is also inverted to accentuate this pattern. Both records show a high frequency component with inter-annual variability, but they also show near-decadal scale variability.

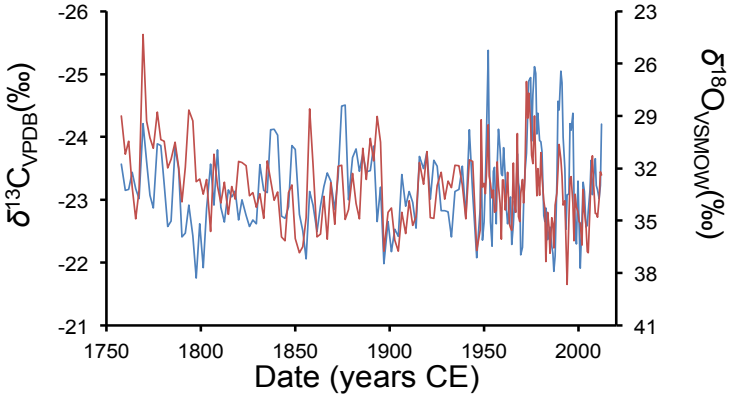

Figure 3. $\delta^{13}C$ (red, left y-axis) and $\delta^{18}O$ (blue, right y-axis) from the Mabuasehube *Vachellia erioloba.* The $\delta^{13}C$ y-axis is inverted to intuitively represent a rainfall proxy scale with high rainfall at the top of the graph and low rainfall at the bottom (see **Figure 4**). The $\delta^{18}O$ y-axis is also inverted to highlight the co-variance with $\delta^{13}C$.

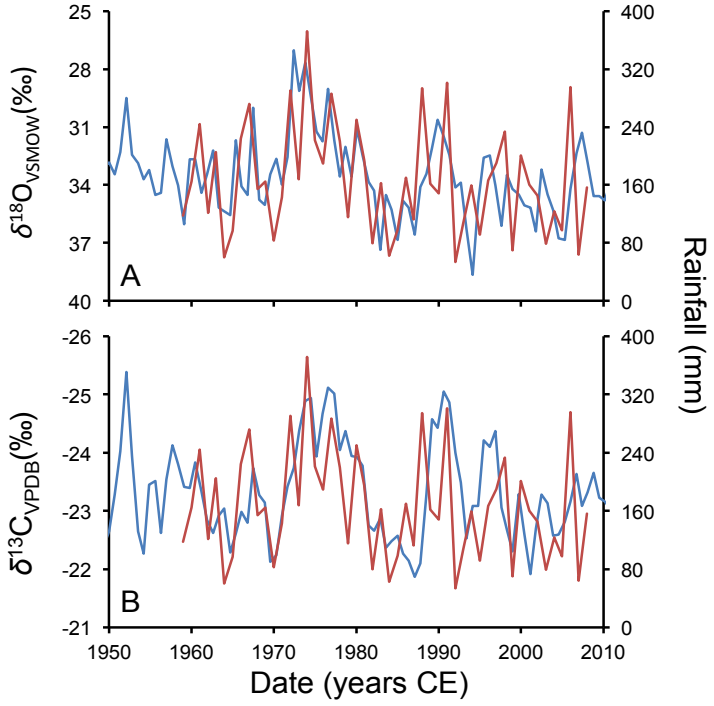

Figure 4. A: The measured $\delta^{18}O$ values, and B: $\delta^{13}C$ values (both blue, left y-axes) show a strong covariance with rainfall (red, right y-axes) from the stations at Tshane and Tsabong [3] (r=-0.778 for $\delta^{18}O$ and r= -0.668 for $\delta^{13}C$). Note that the isotope y-axes are inverted.

Wood $\delta^{18}O$ values typically respond to variations in the isotopic value of source water, or to leaf-level evaporation [27]. In southern Africa the amount effect has been shown to be relatively weak [28] (although this study was done in the winter rainfall area which is distinct from the summer rainfall system at Mabuasehube), while leaf-level evaporation mediated by temperature is dominant [29]. In the summer rainfall area low rainfall and high temperatures coincide and these effects reinforce one another in respect of $\delta^{18}O$ values. The area of the Kalahari Desert from which this tree was sampled is sparsely populated and local rainfall records are rare. We made use of published rainfall records from Tshane, located 115 km north of the sampling site, and Tsabong, located 115 km south of the site [3]. The rainfall from these two sites was averaged to account for the localized variability in convective rainfall in southern Africa [11]. Despite potential problems with the age model based on the assumption of linear radial growth rates the result shows a significant correlation between rainfall and $\delta^{18}O$ values (**Figure 4A**) ($r=-0.778$, $p<0.001$, $n=48$). Irrespective of the role of leaf-level evaporation, and source water effects, this indicates that wood $\delta^{18}O$ values are controlled by rainfall.

The relationship between $\delta^{13}C$ values in wood, and environmental drivers may be affected by a number of variables [27]. In open savanna environments with high ambient growing season temperatures it is anticipated that the dominant factor with be edaphic water availability. In order to verify this the $\delta^{13}C$ record is compared with local rainfall (**Figure 4B**). In the Mabuasehube *Vachellia erioloba* record rainfall is significantly correlated with the $\delta^{13}C$ record ($r=-0.668$, $p<0.0001$, $n=48$), and it suggests that the water-use physiology of *Vachellia erioloba* responds to rainfall, and is reflected in the wood $\delta^{13}C$ values.

The significant empirical correlations between the $\delta^{13}C$ and $\delta^{18}O$ isotopic time series from the Mabuasehube *Vachellia erioloba* specimen and instrumental rainfall records accords with theoretical expectations of stomatal water regulation on $\delta^{13}C$ and source water effects on $\delta^{18}O$. Both isotopic time series proxy rainfall, but the correlation between the $\delta^{13}C$ and $\delta^{18}O$ is not perfect. This is likely the effect of leaf-level evaporation that will affect the $\delta^{18}O$ record, but not the $\delta^{13}C$ record. We conclude that the 255-year rainfall proxy record from the Mabuasehube *Vachellia erioloba* specimen has the potential to provide a basis for assessing long-term climate forcing that cannot be assessed using the short duration instrumental record for the region.

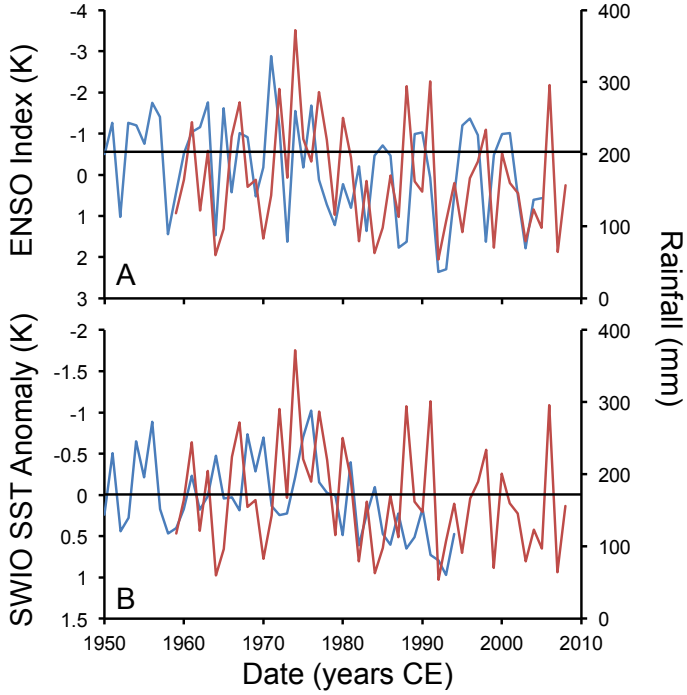

Figure 5. A: Comparison between the instrumental rainfall record (red, right axis) and the ENSO index of Li et al. [30] (blue, left axis). B: instrumental rainfall (red, right axis) and SWIO SST [31] (blue, left axis). Note inverted y-axes in order for the indices to be associate with high rainfall at the top of each plot.

The forcing of rainfall in southern Botswana is reflected in the covariance between the instrumental rainfall records with the indices for ENSO [30] and SWIO SST [31]. While the effect of ENSO (**Figure 5A**) appears to show some intuitive correspondence with rainfall, with positive ENSO index values (that reflect El Niño events) associated with drought conditions, the correlation is not significant ($r=-0.191$, $p=0.120$, $n=47$). Similarly, the correspondence between SWIO SST and the instrumental rainfall record (**Figure 5B**) indicates that warm SST anomalies are associated with drought conditions, but again the correlation is not significant ($r=-0.067$, $p=0.698$, $n=36$). This reaffirms that there is a strong interactive relationship between ENSO and SWIO SST in forcing rainfall in southern Botswana, and that these forces occasionally reinforce one another, and on other occasions act against one another. The instrumental record is not of sufficient duration to be able to determine the interactive modulation of these drivers.

When the covariance between the isotopic proxies and the indices for ENSO and SWIO SST are considered, the dataset provides insight in to the long-term rainfall forcing. As was noted for the instrumental data, there is a strong indication that El Niño is associated with drought and La Niña with wet conditions in both the $\delta^{18}O$ (**Figure 6A**) and the $\delta^{13}C$ records (**Figure 6C**).

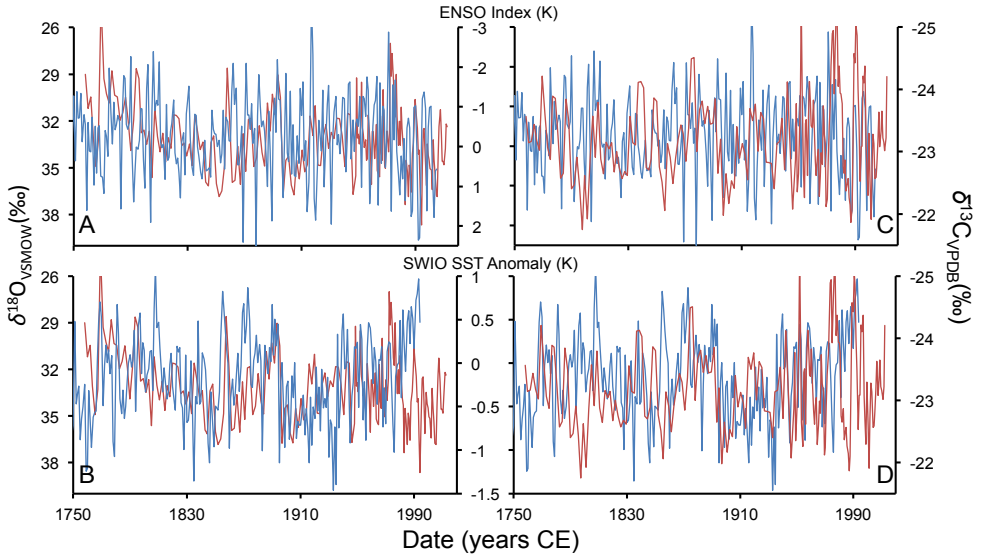

Figure 6. Comparison between isotope records from the Mabuasehube *Vachellia erioloba* and reconstructions of forcing parameters. A: comparison between the $\delta^{18}O$ record and the ENSO index of Li et al. [30]. B: comparison between the $\delta^{18}O$ record and the SWIO SST anomaly record of Zinke et al. [31]. C & D: similar comparisons to A & B using the $\delta^{13}C$ record. Isotopic records are depicted in red, and the ENSO and SWIO SST indices are depicted in blue. Note some y-axes are inverted to depict high rainfall at the top of each plot and low rainfall at the bottom.

In the case of $\delta^{18}O$ the correlation with ENSO is significant (r=0.387, p=0.007, n=56), but the correlation is insignificant when using the $\delta^{13}C$ record (r=-0.012, p=0.931, n=56). The correlation between the $\delta^{18}O$ record and SWIO SST is marginally significant (r=0.355, p=0.027, n=45), but with the $\delta^{13}C$ record is insignificant (r=-0.020, p=0.899, n=45) (**Figure 6B** and **Figure 6D**).

The effect that SWIO SST has on rainfall appears to have changed from a positive correlation in which increased SST leads to increased rainfall (**Figure 5B**), to a negative correlation in which the opposite is true (**Figure 6B** and **Figure 6D**). The transition seems to take place in about 1980 CE. In an

analysis of instrumental rainfall records across Botswana, Mphale et al. [3] also noted a breakdown in the relationship between SST and rainfall and between ENSO and rainfall. These authors identified the date threshold for this change as 1982 CE, and attributed it to an eastward shift of the main rainfall bearing synoptic system that led to a significant reduction in rainfall at this time. Woodborne et al. [11] also mooted an east/west shift in the synoptic system to explain isotopic proxy rainfall records from baobabs in the Mapungubwe and Pafuri areas of South Africa (**Figure 1**). The proposed mechanism suggested that warmer SST drives eastward displacement of the temperate tropical troughs that are responsible for most of the Austral summer rainfall in the region [32]. The mechanism predicts that Botswana should become drier when SST increases. The evidence from the Mabuasehube *Vachellia erioloba* specimen appears to run counter to this as prior to 1980 CE increased SST is associated with higher rainfall (**Figure 6B** and **Figure 6D**).

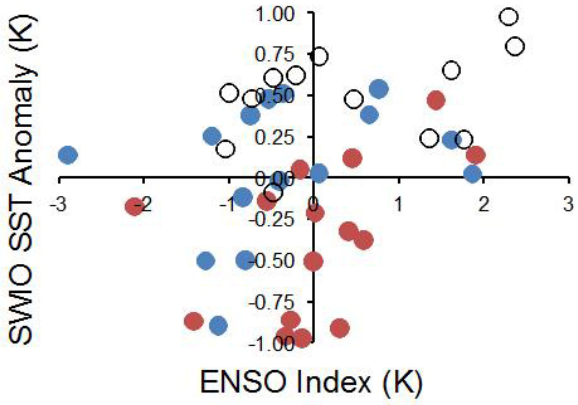

Figure 7. Rainfall forcing of wet and dry years. The 15 wettest years (blue symbols) pre-1980 CE are associated with positive SWIO SST anomalies [31] or negative ENSO indices [30] (La Niña conditions). The 15 driest years pre-1980 CE (red symbols) are associated with negative SWIO SST anomalies or positive ENSO indices (El Niño conditions). The post-1980 CE period (open symbols) is dominated by strong El Niño conditions with weak interleaved La Niña conditions, and an unprecedented warming of the SWIO SST. Both wet and dry conditions prevailed but the period is generally drier and ENSO is the dominant forcing (**Figure 5A**).

The evidence presents a conundrum in which the role of ENSO appears to be relatively coherent with El Niño associated with drought and La Niña with wet conditions, but the modulating effect of SWIO SST changes through time. To unravel the knot, it is necessary to have long-term data.

We divided the record in to pre- and post-1982 CE, and then ranked the pre-1982 CE record from wettest to driest years using the $\delta^{18}O$ record, which is the most consistent indicator of rainfall in the foregoing analysis. We analysed the ENSO and SWIO SST conditions that prevailed during the 15 wettest and 15 driest years pre-1980 CE and compared them with the conditions that have prevailed post-1980 CE (**Figure 7**).

Pre-1980 CE the wet conditions (blue symbols in **Figure 7**) were associated with either negative ENSO index values (La Niña conditions), or with positive SWIO SST anomalies. It is important to note that El Niño events are included in the portfolio of wet years. Conversely positive SWIO SST anomalies alone do not determine wet conditions. Pre-1980 CE the dry conditions (red symbols in **Figure 7**) are dominated by positive ENSO index values (El Niño conditions) or negative SWIO SST anomalies. Again La Niña conditions are among the droughts, but these were associated with negative SWIO SST anomalies. The evidence suggests that both ENSO and SWIO SST played an important role in modulating rainfall, and when ENSO and SWIO SST anomalies have the opposite signs they reinforce one another to produce definitive drought (+ ENSO, - SWIO SST) or definitive wet (- ENSO, + SWIO SST) conditions. The highest uncertainty is when both ENSO and SWIO SST indices have the same sign. Under these conditions ENSO and SWIO SST act against one another, and there is no pattern to indicate whether the wet or the dry forcing will dominate.

The post-1980 CE period represents the most persistent dry conditions across Botswana since 1950 CE [3]. This is also patent in the isotope proxy records for the last 255 years (**Figure 3**, **Figure 6**). The post-1980 CE period is characterized by an unprecedented positive shift in the SWIO SST, which shows only positive indices for this period (**Figure 7**). It also has a high frequency of intense El Niño interspersed with weak La Niña conditions. In the pre-1980 CE period positive SWIO SST anomalies appear to have facilitated wet conditions, but in the post-1980 CE period the ENSO signal is the dominant force (**Figure 5A**) resulting in drier conditions because of the frequency and intensity of El Niño events.

CONCLUSIONS

Mphale et al. [3] suggested that rainfall has decreased over Botswana over the last 50 years; but the 250-year record from the Mabuasehube *Vachellia erioloba* specimen shows no significant trend over the longer period. Instead our analysis suggests that a post-1980 CE decline in average rainfall is the result of interactive ENSO and SWIO SST forcing of rainfall. The frequency and intensity of El Niño events has been the dominant effect since 1980 CE.

The analysis also shows that east/west shifts of the temperate tropical trough synoptic systems that have been invoked to explain wet/dry cycles at Pafuri and Mapungubwe [11] are not supported by the Botswana evidence. The temperate tropical trough system is responsible for the majority of the summer rainfall over southern Africa, and a coherent response across the entire region would be expected. Dry conditions at Mapungubwe and Pafuri during periods of elevated SWIO SST were attributed to an eastward shift of the temperate tropical trough system, and should have led to hyper-arid conditions in Botswana. Instead the Mabuasehube *Vachellia erioloba* record indicates wetter conditions with elevated SWIO SST. The evidence suggests an alternative possibility: that the temperate tropical trough system shifts westward during positive SWIO SST anomalies. This scenario would still lead to drier conditions at Mapungubwe and Pafuri, but wetter conditions in Botswana.

This study demonstrates that the $\delta^{13}C$ and $\delta^{18}O$ values in the wood of *Vachellia erioloba* yield records of rainfall variability. Since this species achieves great age, and is widely distributed in the xeric regions of the Kalahari and Namib Deserts, it holds the potential to elucidate past climate where instrumental records are rare. Additional specimens from across the arid Kalahari Desert, including the possibly of sampling longer-lived specimens, will clarify the patterns that have been tentatively identified in this study.

EXPERIMENTAL SECTION

Sample collection. Permission to sample trees in Botswana was obtained from the Ministry of Environment, Wildlife and Tourism under permits reference EWT8/36/4CCVIII (18) and (28). A *Vachellia erioloba* specimen was identified in the Mabuasehube Game Reserve in southern Botswana (25°05'52.36"S, 21°59'47.80"E) (**Figure 1**). The tree was selected because it had recently died (indicated by bark loss and absence of leaves, while still retaining some of the fine branch structures). It was located in an area with a sandy substrate with no evidence of drainage lines so that edaphic moisture is regulated by rainfall. In 2015 a disk was removed from the stem using a chainsaw and imported in to South Africa under a permit P0073346 issued by the South Africa Department of Agriculture, Forestry and Fisheries.

Sample preparation. A radial section of approximately 1 cm width, which included all the growth rings pith to bark, was removed from the disk. In order to curate a witness section, the sample radius was mounted between pinewood backing blocks using water-soluble glue, and then split to produce mirror image sections. These sections were archived until required for this analysis. For the analysis the glue was removed from the analysis section

by soaking it in hot water for two hours. As the wood was extremely hard, *ca.* 1 mm slivers were cut using a chisel and a modified wood plane. A total of 196 aliquots were removed along the 243 mm radius.

Isotopic analysis. Lignin was oxidised with acidified sodium chlorite and the hemicelluloses were subsequently hydrolysed with sodium hydroxide to yield α-cellulose [33, 34] that was homogenized using a Hielscher ultrasonic probe [35]. The samples were freeze-dried in a Thermo Savant ModulyoD freeze drier at -45°C for at least 48h. Aliquots of 0.30–0.35 mg of α-cellulose were weighed into silver capsules and pyrolyzed over glassy carbon at a temperature of 1,090°C in a PDZ Europa ANCA GSL elemental analyser interfaced to a PDZ Europa 20–20 stable isotope ratio mass spectrometer. Isotope ratios are expressed as per mille deviations using the standard delta notation relative to VPDB (carbon) and VSMOW (oxygen) standards. Analytical precision was typically ±0.1‰ for carbon and ±0.3‰ for oxygen.

Data corrections. The $\delta^{13}C$ record was corrected for changes in the $\delta^{13}C$ of atmospheric CO_2 using the southern Hemisphere record of [36] with online updates of the dataset (http://cdiac.ornl.gov/ftp/db1014/isotope.cgo). The correction of the $\delta^{13}C$ record to account for increased atmospheric CO_2 concentration was done using the approach of Woodborne et al. [11, 23].

Dating and calibration. Dating samples were taken from the residual material from the isotopic analysis and since these were processed to the level of α-cellulose no additional pretreatment was required. Three samples were selected, with two chosen to fall within the bomb carbon period. Samples were measured by Accelerator Mass Spectrometry at iThemba LABS [37]. Calibration was done using the SHcal13 and SHZ1_2 datasets on the online version of CALIBomb (http://calib.org/CALIBomb/) (**Table 1**).

Table 1. Radiocarbon dating results from the Mabuasehube *Vachellia erioloba.*

Sample	Laboratory number	$\delta^{13}C$	pMC	pMC error	Age	Age error	Calibration range (year CE)
41	IT-C-1069	-23.0	123.14	0.53			1962-1963, 1982-1985
44	IT-C-1097	-23.1	124.33	0.47			1962-1963, 1982-1984
93	IT-C-1070	-23.8	97.29	0.39	221	32	1960-1727, 1805-1816, 1832-1892, 1922-1950
192-4 (193)	IT-C-1071	-23.3	96.80	0.42	261	35	1643-1672, 1743-1760, 1762-1770, 1779-1796

Age model construction. An age model was constructed using a linear fit between age and sample number. Samples 41 and 44 (samples numbers increased from the bark towards the centre of the tree) both contained bomb carbon with sample 44 having a higher percent modern carbon value indicating that the descending section of the bomb calibration curve applied. This leaves little latitude for the age assignment, and the linear age model was extrapolated to intercept the 1-sigma calibration range of the third date (sample 92). This linear extrapolation implies that that the termination of growth took place in 2013, which is consistent with the death of the tree within a year or two of the sampling in 2015.

The radiocarbon date on the inner ring (sample 193) indicates that the growth rate of the Mabuasehube *Vachellia erioloba* was not constant through time and the linear age model spanning samples 0-93 does not intersect with the 1-sigma age range for sample 193. A separate linear extrapolation of age was used for samples 93-194 using the most probable calibrated age for sample 193. The age model patently includes inaccuracies because of the assumption of linear growth, and assuming a single inflection point for the change in growth rate. Year-to-year variation in environmental conditions will lead to faster and slower growth, which manifests as errors in the age model. As a result it is acknowledged that the age model approximates average growth and cannot be used to assign the year of growth for individual samples.

Statistical analysis. The statistical comparison of the time series was done using the KNMI Climate Explorer online tools (http://climexp.knmi.nl/userseries.cgi) accessed 30 December 2017. Rainfall derived from convective systems is spatially variable: the comparison between the two instrumental records used in this study, from Tshane and Tsabong, does not yield a perfect correlation ($r=0.639$, $p<0.001$, $n=50$). The statistical comparison between rainfall proxies and instrumental records need to account for this. In addition the approach used to construct the age model does not have sufficient precision to assign an isotope measurement to a growth year with high levels of confidence. The local variability in rainfall and the lack of precision in the age model prevent the use of the isotope records in assessing annual scale variability, and a 3-year running average for all parameters is used in the assessment of slightly longer-term forcing effects.

ACKNOWLEDGMENTS

This project was funded by The National Research Foundation (NRF) of South Africa under the Research Grant for Unrated Researchers number CSUR13092647960. AMS radiocarbon analyses were supported by the Romanian Ministry of Research and Innovation CNCS-UEFISCDI under grant PN-III-P4-ID-PCE-2016-0776, Nr. 90/2017.

REFERENCES

1. J. Rockstrom, *Physics and Chemistry of the Earth, Part B: Hydrology, Oceans and Atmosphere,* **2000**, *25*, 275.
2. J. A. Adedoyin, *Meteorology Atmospheric Physics,* **2000**, *75*, 135.
3. K. M. Mphale, S. K. Dash, A. Adedoyin, S. K. Panda, *Theoretical and applied climatology*, **2014**, *116*(1-2), 75.
4. M. Hoerling, J. Hurrell, J. Eischeid, A. Phillips, *Journal of Climate*, **2006**, *19*(16), 3989.
5. S. E. Nicholson, D. Leposo, J. Grist, *Journal of Climate*, **2001**, *14*, 323.
6. D. J. Nash, G. H. Endfield, *Climatic Change*, **2008**, *86*(3-4), 257.
7. R. Neukon, D. J. Nash, G. H. Enfield, S. W. Grab, C. A. Grove, C. Kelso, C. H. Vogel, J. Zinke, *Climate Dynamics*, **2013**, DOI 10.1007/s00382-013-1886-6
8. Y. Richard, S. Trzaska, P. Roucou, M. Rouault, *Climate Dynamics*, **2000**, *16*(12), 883.
9. L. Gimeno, A. Drumond, R. Nieto, R. M. Trigo, A. Stohl, *Geophysical Research Letters*, **2010**, *37*(13).
10. N. Fauchereau, B. Pohl, C. J. C. Reason, M. Rouault, Y. Richard, *Climate Dynamics*, **2009**, *33*(4), 575.
11. S. Woodborne, P. Gandiwa, G. Hall, A. Patrut, J. Finch, *PloS one*, **2016**, *11*(7), p.e0159361.
12. P.D. Tyson, G. R. J. Cooper, T. S. McCarthy, *International Journal of Climatology,* **2002**, *22*(9), 1105.
13. F. A. Engelbrecht, W. A. Landman, C. J. Engelbrecht, S. Landman, M. M. Bopape, B. Roux, J. L. McGregor, M. Thatcher, M., *Water SA*, **2011**, *37*(5), 647.
14. F. Engelbrecht, J. Adegoke, M. J. Bopape, M. Naidoo, R. Garland, M. Thatcher, J. McGregor, J. Katzfey, M. Werner, C. Ichoku, C. Gatebe, *Environmental Research Letters*, **2015**,*10*(8), p.085004.
15. H. H. Shugart, S. A. Macko, P. Lesolle, T. A. Szuba, M. M. Mukelabai, P. Dowty, R. J. Swap, *Global Change Biology*, **2004**, *10*(3), 273.
16. D. W. Stahle, P. T. Mushove, M. K. Cleaveland, F. Roig, G. A. Haynes, *Forest Ecology and Management*, **1999**, *124*(2), 217.
17. M.D. Therrell, D. W. Stahle, L. P. Ries, H. H. Shugart, *Climate Dynamics*, **2006**, *26*(7-8), 677.
18. M. Hall, *Annals of the Natal Museum*, **1976**, *22*(3), 693.
19. J. C. Vogel, A. Fuls, E. Visser, *South African Journal of Science*, **2001**, *97*(3-4), 164.
20. J. F.Thackeray, S. Potze, *Annals of the Transvaal Museum,* **2000**, *37*, 131.
21. P. D. Dunwiddie, V. C. LaMarche, *Nature*, **1980**, *286*(5775), 796.
22. G. Hall, S. Woodborne, M. Pienaar, *The Holocene*, **2009**, *19*(2), 251.
23. S. Woodborne, G. Hall, I. Robertson, A. Patrut, M. Rouault, N. J. Loader, M. Hofmeyr, *PLoS One*, **2015**, *10*(5), p.e0124202.

24. E. Norström, K. Holmgren, C. M. Morth, *South African Journal of Science*, **2005**, *101*(3-4), 162.
25. S. Woodborne, S., 2004. *CSIR Environmentek,* **2004**. Available from author.
26. T. H. Wils, I. Robertson, S. Woodborne, G. Hall, M. Koprowski, Z. Eshetu, *Journal of Quaternary Science*, **2016**, *31*(4), 386.
27. D. McCarroll, N. J. Loader, *Quaternary Science Reviews*, **2004**, *23*(7), 771.
28. C. Harris, C. Burgers, J. Miller, F. Rawoot, *South African Journal of Geology*, **2010**, *113*(1), 33.
29. O. W. Cape, *South African Journal of Science*, **1997**, *93*.
30. J. Li, S. P. Xie, E. R. Cook, G. Huang, R. D'arrigo, F. Liu, J. Ma, X. T. Zheng, *Nature Climate Change*, **2011**, *1*(2), 114.
31. J. Zinke, B. R. Loveday, C. J. C. Reason, W. C. Dullo, D. Kroon, *Scientific reports*, **2014**, *4*, 4393.
32. M. S. J. Harrison, *International Journal of Climatology*, **1984**, *4*(5), 547.
33. N. J. Loader, I. Robertson, A. C. Barker, V. R. Switsur, J. S. Waterhouse, *Chemical Geology*, **1997**, *136*(3-4), 313.
34. K. T. Rinne, T. Boettger, N. J. Loader, I. Robertson, V. R. Switsur, J. S. Waterhouse, *Chemical Geology*, **2005**, *222*(1), 75.
35. W. Laumer, L. Andreu, G. Helle, G. H. Schleser, T. Wieloch, H. Wissel, *Rapid Communications in Mass Spectrometry,* **2009**, *23*, 1934.
36. R. J. Francey, C. E. Allison, D. M. Etheridge, C. M. Trudinger, I. G. Enting, M. Leuenberger, R. L. Langenfelds, E. Michel, L. P. Steele, *Tellus B*, **1999**, *51*(2), 170.
37. V. L. Mbele, S. M. Mullins, S. R. Winkler, S. Woodborne, *Physics Proceedia*, **2017**, *90*, 10.